Cytoskeleton Network and Cellular Migration Modulated by Nuclear-localized Receptor Tyrosine Kinase ROR1

HSIAO-CHUN TSENG[1,2], HSIAO-WEI KAO[2], MENG-RU HO[2],YET-RAN CHEN[3], TIN-WEI LIN[3], PING-CHIANG LYU[1] and WEN-CHANG LIN[2]

[1]*Institute of Bioinformatics and Structural Biology, National Tsing Hua University, Hsinchu, Taiwan, R.O.C.;*
[2]*Institute of Biomedical Sciences, Academia Sinica, Taipei 115, Taiwan, R.O.C.;*
[3]*Agricultural Biotechnology Research Center, Academia Sinica, Taipei 115, Taiwan, R.O.C.*

Abstract. *Biological functions of receptor tyrosine kinase-like orphan receptor 1 (ROR1) remain to be elucidated due to the lack of identified genuine ligands. Previously, transiently expressed ROR1 was unexpectedly found to exhibit nuclear localization, the functions of which are unknown. Materials and Methods: We constructed nuclear-homing peptidyl-prolyl cis-trans isomerases (FKBP) domain fusion ROR1-expressing cells and used a synthetic dimerizer to specifically activate FKBP-fused ROR1 proteins for subsequent functional characterization. Results: Activation of nuclear-homing ROR1 by treating cells with AP20187 dimerizer led to significant increase in actin stress fibers and increased cellular migration. Following gene expression microarray analysis, we demonstrated that activated ROR1 affects several genes involved in the regulation of the actin cytoskeleton (radixin (RDX), ezrin (EZR), son of sevenless homolog 2 (SOS2) and caldesmon 1 (CALD1)). Conclusion: Our data indicate that nuclear-localized ROR1 may play an important role in cell migration and cytoskeleton remodeling. This might explain the critical roles of ROR1 in neuron development.*

Recent investigations have demonstrated the unanticipated nuclear localization of receptor tyrosine kinases (RTKs) in addition to their typical cell membrane localization. These include those of the epidermal growth factor receptor (EGFR) family (EGFR (1), ERBB-2 (2), ERBB-3 (3), ERBB-4 (4)), the fibroblast growth factor receptor (FGFR) family [FGFR1 (5, 6), FGFR3 (7)], neurotrophic tyrosine kinase, receptor, type 1 (TRKA) (8) and vascular endothelial growth factor receptor 2 (VEGFR2) (9). The biological significance of nuclear-localized RTKs is not fully known. Studies pioneered from Dr. Mien-Chie Hung's group at M.D. Anderson Cancer Center have implicated the transactivation capability of these nuclear-localized RTKs, aside from their typical enzymatic kinase activity (10). It is not known how many RTKs may have nuclear localization potential. To survey the nuclear localization possibility of all twenty families of human RTKs overall, bioinformatic analyses were performed to predict nuclear-homing potential. Besides the well-studied EGFR and FGFR families, our predictions showed additional RTKs, including receptor tyrosine kinase-like orphan receptors (ROR1 and ROR2), could be localized in the nucleus (11).

ROR1 and ROR2 are type I membrane proteins and belongs to the ROR subfamily of cell surface receptors. They are characterized by the extracellular Frizzled-like cysteine-rich domains (CRDs) and Kringle domains, in addition to their intracellular tyrosine kinase domain (12) and they possess possible functions in mammalian central neuron development (12, 13). The ROR proteins are expressed during synapse formation and concentrated in the growth cone of the immature neuron (14). RORs are evolutionally conserved among *Caenorhabditis elegans*, *Aplysia*, *Drosophila melanogaster*, *Xenopus,* mice, and humans (15, 16). Mutations in the *Ror* gene of *C. elegans* cause inappropriate axon outgrowth, as well as defects in cell migration and asymmetric cell division. In addition, knockdown of *Ror1* or *Ror2* expression leads to a shorter and less branched neurite extension (13). ROR1 associates with microfilament construed by F-actin, whereas ROR2 co-localizes with microtubules (17), suggesting that ROR1 and ROR2 have different subcellular localization, which could imply a possible functional modulation inside cells.

No biological ligands have been identified thus far for the ROR1 RTKs. Therefore, it is challenging to study the downstream activation signaling of ROR1 in the absence of identification of genuine ligands. Many receptor proteins are generally activated or triggered by the induced interaction, or

Correspondence to: Wen-chang Lin, Institute of Biomedical Sciences, Academia Sinica, Taipei 115, Taiwan, R.O.C. Tel: +886 226523967, Fax: +886 227827654, e-mail: wenlin@ibms.sinica.edu.tw

Key Words: Actin cytoskeleton, cell migration, nuclear localization, ROR1, receptor tyrosine kinase.

dimerization, of their cognate ligands. In order to examine the function of such an orphan receptor (ROR1), we has applied the ARGENT™ regulated homodimerization system (ARIAD, MA, USA). This system utilizes the FK 506 binding domains (FKBP36v) and synthetic chemical dimerizers. FKBP is an abundant cytoplasmic protein that serves as the initial intracellular target for the immunosuppressive drug FK506 (18). Based on the structure of FK506, synthetic chemical analog AP20187 is designed to dimerize FKBP fusion proteins of interest and thus can be used to activate orphan receptor kinases, like ROR1. AP20187 is a cell-permeant organic molecule with two separate motifs that each bind with high affinity to $FKBP_{36v}$ domain (19, 20). FKBP36v is a modified FKBP with a single amino acid substitution, Phe36Val (FV), which has 1000-fold higher binding affinity to AP20187 than the wild-type protein.

From previous study, wild-type ROR1 protein can be localized both in the nucleus and membrane compartments. In order to specifically examine the putative functional roles of only nuclear localized ROR1 in the cells, we constructed $FKBP_{36v}$ fusion ROR1 construct containing $NLS^{c\text{-}MYC}$ (N-ROR1) for nuclear targeting. The $FKBP_{36v}$ fusion ROR1 was stably expressed under doxycycline repression system in HeLa TF tet-off cells. This cell line was chosen not only for its doxycycline/tetracycline-regulated transcription control ability but also for the low expression level of endogenous ROR1 (data not shown). In order to systematically examine the global cellular responses by nuclear localized ROR1 activation, we used whole-genome microarray expression analysis in N-ROR1-expressing cells to analyze alterations in gene expression following ROR1 activation.

Materials and Methods

Plasmid construction. The human ROR1 cytoplasmic part was subcloned into the *Xba*I site of the pC_4-F_v1E vector (ARIAD, MA, USA). The F_v1 fused human ROR1cytoplasmic fragment was released and then subcloned into the pC_4-F_v1E vector again to generate two copies of Fv (Fv2). In addition, the synthesized $NLS^{c\text{-}MYC}$ linker was inserted into the *Spe*I site. For expression, the FKBP fusion ROR1 protein region was subcloned into the *Mlu*I and *Not*I site downstream of the Tet-responsive P_{hCMV} promoter of pTRE2pure (Clontech, CA, USA). The resulting N-ROR1 plasmid (Figure 1) was verified by DNA sequencing and Western blotting to confirm the correct expression of the fusion protein.

Cell culture and transfection. HeLa Tet-Off (HeLa TF) cells were obtained from Clontech and grown in DMEM (Life Technologies, Inc., CA, USA), supplemented with 10% fetal calf serum, and 1% penicillin-streptomycin. This is a human cervical epithelioid carcinoma-derived cell line that expresses the tetracycline-controlled transactivator (tTA). To generate stable cell lines, these cells were transfected using Lipofectamine™ 2000 (Invitrogen, CA, USA) with expression plasmids pTRE2pure_F_v2$NLS^{c\text{-}MYC}$E_cyto. ROR1. By puromycin selection, several positive clones were screened for nuclear localized ROR1 expression (N-ROR1 clones). All experiments were performed using the selected N-ROR1 (c2) clone for each condition. To suppress ROR1 expression, cells were treated with 0.1 μg/ml doxycycline for 24 hours to control the CMV promoter activity.

RNA extraction and RT-PCR. Total RNA was extracted using TRIzol Reagent (Invitrogen) according to the manufacturer's protocol. Reverse transcription was performed in 20 μl reaction volume containing 5 μg of sample RNA, 200 U of SuperScript™ III reverse transcriptase, 2.5 μM of oligo (dT)15, 500 μM dNTP mix, 5 mM DTT (Invitrogen), and 1× First-strand Buffer (Invitrogen). Tubes were incubated at 50˚C for 1 hour and then at 70˚C for 15 minutes to terminate the reaction. The amplification program includes denaturation of 95˚C for 10 minutes, followed by 40 cycles at 95˚C for 15 seconds, and 60˚C for 1 minute. Amplification was followed by melting curve analysis using the program run for one cycle at 95˚C for 15 seconds, 60˚C for 1 minutes and 95˚C 15 seconds. The real-time PCR was performed using gene-specific primers. The following primer sets were used: Caldesmon (CALD1)-139-F1: 5'-CAGGAACGGCTGCGGCAGAA and Caldesmon (CALD1)-296-R1: 5'-CGCTCCAGGAATGCGGCCTC for specifically recognized *CALD1* expression; son of sevenless homolog 2 (SOS2)-3704-F1: 5'-AGCCACCTCCACTGGGGCAT and son of sevenless homolog 2 (SOS2)-3951-R1: 5'-GGGGTG CGAAAGCTCCCGTT for specifically recognized *SOS2* expression; ezrin (VIL2 (EZR))-363-F1: 5'-TGCCGTGCTCTTGGGGTCCT and ezrin (VIL2 (EZR))-547-R1: 5'-GCATCCCACGGTGTTCCGCA for specifically recognized *VIL2* (*EZR*) expression; radixin (RDX)-1176-F1: 5'-GCGTCGAGCTGCTG AAGAGGC and a radixin (RDX)-1433-R1: 5'-ACTGGTGGTGGTG GAGGTGGA for specifically recognized *RDX* expression; and glyceraldehyde-3-phosphate dehydrogenase (GAPDH)-1F (5'-TGGTATCGTGGAAGGACTCA-3'), glyceraldehyde-3-phosphate dehydrogenase (GAPDH)-2R (5'-AGTGGGTGTCGCTGTTGAAG-3') corresponding to coding sequence 504-874 of the *GAPDH* human sequence. The reaction products were then subjected to PCR amplification. PCR products were separated by electrophoresis on 1.5% agarose gels in Tris, acetic acid and EDTA (TAE) buffer (Invitrogen) and visualized with ethidium bromide staining (21).

Microarray experiments and data analysis. For identifying genes regulated by N-ROR1, N-ROR1 (c2) cells were treated with doxycycline (0.1 μg/ml) as negative control in which N-ROR1 expression was suppressed, and N-ROR1 (c2) cells were treated with AP20187 for 0, 1, 12 and 24 hours in which N-ROR1 expression were induced. Total RNA was isolated from the treated N-ROR1 (c2) cells and subsequently used for microarray analysis using HG-U133plus2 Gene Chip (Affymetrix, Santa Clara, CA, USA). This array experiment was performed at the NRPGM Microarray & Gene Expression Analysis Core Facility at the National Yang-Ming University School. For preliminary selection criteria, we selected genes with expressions that differed by a factor of at least 1.3-fold with respect to the control reference. Control reference was the average of the gene expression intensities from the two samples including N-ROR1 (c2) cells treated with doxycycline (N-ROR1 expression suppressed) and N-ROR1 (c2) cells treated with ethanol (vehicle control). Experimental samples were the average of the intensities from the three samples including N-ROR1 (c2) cells treated with AP20187 for 1, 12, and 24 hours, respectively. Genes were then filtered by eliminating those that had no signal in the sample from N-ROR1 (c2) cells treated with AP20187 for 24 hours. This resulted in a total of 2012 genes for subsequent analysis. An

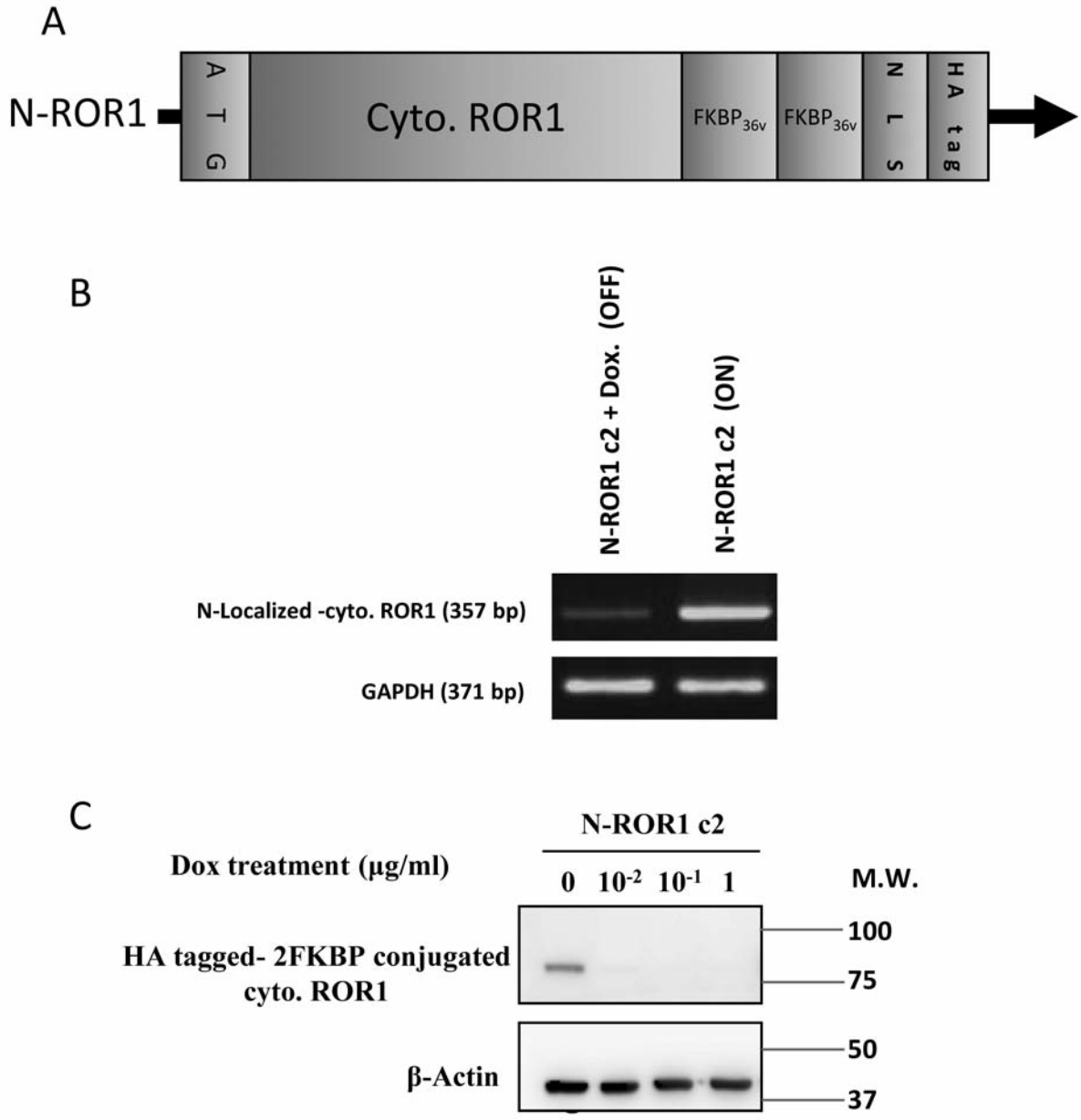

Figure 1. *Establishment of N-ROR1 (c2) cells. ROR1 expression is modulated by doxycycline (dox) in transfected cells. Nuclear localized ROR1 was induced in N-ROR1 (c2) cells in the absence of doxycycline. In the presence of doxycycline (Tet-OFF), ROR1 expression was abolished. A: Schematic illustration of $FKBP_{36v}$ fused cyto. ROR1 construct used for transfection. B: RT-PCR analysis of ROR1 transcript revealed that expression only occurred in induced N-ROR1 (c2) cells and suppression of expression occurred with doxycycline (Tet-OFF). C: N-ROR1 protein expression of N-ROR1 (c2) cells. Cell lysates were extracted for analysis of the expression of N-ROR1 proteins with or without doxycycline suppression.*

Expression Analysis Systematic Explorer (EASE) cluster analysis was applied to the group of genes on the basis of the same Kyoto Encyclopedia of Genes and Genomes (KEGG) pathway. A hierarchical clustering method was applied to groups of genes and samples on the basis of the similarities in expression, and the analyses were visualized using Multiple Array Viewer software (http://www.tm4.org/). The approach to analyzing this data set relied on the clustering method, self-organizing maps (SOM).

Immobilized metal affinity chromatography (IMAC) purification of phosphopeptides and peptide identification using liquid chromatography–mass spectrometry (LC-MS). To purify all the cellular phosphopeptides, a homemade Fe^{3+}-NTA IMAC column was used. The IMAC column was prepared by packing Ni-NTA resin (QIAGEN Inc., CA, USA) into a 500 μm ID × 5 cm PEEK™ tubing. The column was then attached to an HPLC pump with a continuous flow (13 μl/min) of loading buffer (6% acetic acid with pH 3.5). The

Ni^{2+} was removed from the resin by injection of 100 μl of 50 mM EDTA with 1 M NaCl (pH 9.0) into the column, followed by charging the ferric ion using 100 μl of 100 mM $FeCl_3$. The resin was washed with loading buffer for 15 minutes to remove excess ferric ion and the column was ready for phosphopeptide purification. To purify the phosphopeptides, the peptide mixture dissolved in 6% acetic acid (pH 3.0) was injected into the IMAC column and then the column was sequentially washed with 300 μl loading buffer, 100 μl 30% (v/v) acetonitrile and 300 μl loading buffer. Finally, the phosphopeptides were eluted by injection of 100 μl of 200 mM $NH_4H_2PO_4$ (pH 4.4) into the IMAC column. The eluted phosphopeptide mixture was concentrated by vacuum centrifugation and cleanup was carried out using Zip-Tip (Millipore, MA, USA). The purified phosphopeptides were analyzed by an LC-MS system, for which the instrumentation and method were reported previously (22).

Immunocytochemistry. The treated cells seeded on the coverslips were washed with PBS. N-ROR1 (c2) cells were fixed for 15 minutes with 3.7% formaldehyde in phosphate-buffered saline (PBS) and then permeabilized in 0.1% Triton X-100 in PBS for 5 minutes. The coverslips were preincubated in 5% bovine serum albumin (BSA) in PBS for 20 minutes at 37˚C and exposed to the primary antibodies (diluted in 1% BSA + 0.1% Triton X-100 in PBS) for 1 hour at 37˚C. Finally, the cultures were rinsed three times in PBS for 3 minutes and incubated with secondary antibodies for 1 hour at 37˚C. After secondary antibody incubation, the cultures were washed three times in PBS for 10 minutes and then preserved in mounting medium (Vector, CA, USA). The following primary antibody was used: HA.11 monoclonal antibody (MMS-101P, dilution 1:150; Covance, NJ, USA); the following secondary antibody was used: anti-mouse IgG fluorescein isothiocyanate (FITC)-conjugated (sc-2099, 1:100; Santa Cruz Biotechnology, CA, USA). To detect actin filaments, cells were stained with phalloidin rhodamine (R415, 1:100; Invitrogen) for 1 hour at 37˚C. As a negative control, one coverslip was incubated without the primary antibody (23).

Results

Establishment of N-ROR1 stable expression clones. In order to examine the novel functional roles of ROR1 localized in the nucleus, we first constructed the $FKBP_{36v}$ fusion ROR1 construct. The N-ROR1 construct contained the cytoplasmic region of *ROR1* gene, two copies of $FKBP_{36v}$ domain, and a $NLS^{c\text{-}MYC}$ region followed by a carboxyl-terminal HA tag (Figure 1A). The modified $FKBP_{36v}$ with higher binding affinity to AP20187 dimerizer allowed us to specifically activate the ROR1 kinase. This homodimerization system from ARIAD has been applied extensively to perform regulated signal transduction activation previously (20). This construct contains an $NLS^{c\text{-}MYC}$ sequence for nuclear targeting expression. Due to the presence of this NLS signal, the fusion ROR1 proteins are targeted mainly to the nucleus.

In a previous study (11), we observed that wild-type ROR1 would distribute both in the nucleus and in cytoplasmic membrane compartments. To reduce the background effects from membrane-anchored ROR1 proteins and simplify downstream function analysis, we opted to use the additional $NLS^{c\text{-}MYC}$ sequence to strengthen nuclear localization of fusion proteins. In addition, the N-ROR1 protein expression is under the control of a doxycycline-inducible promoter, which allowed us to timely regulate the expression of ROR1 fusion protein for microarray experiments. HeLa Tet-Off cells were used for this experiment, so that the expression of fusion ROR1 protein is further under the suppression of doxycycline in the culture medium.

Following transfection of HeLa TF cells with the N-ROR1 construct, recipient cells were grown on medium containing the drug G418 and puromycin. Following the selection process, several clones were isolated and examined for their expression of fusion ROR1 proteins. N-ROR1 (c2) was finally chosen as the functional assay model in this study. The expression of N-ROR1 fusion protein was characterized by RT-PCR (Figure 1B) and western blot analyses (Figure 1C). The expected protein localization was validated by an immunofluoresence microscopy analysis (Figure 2A). As expected, the N-ROR1 proteins were mainly localized in the cell nucleus following the release of doxycycline.

Gene expression profiling following the N-Ror1 activation. In order to identify gene expression alterations following the specific activation of N-ROR1 in the nucleus, we designed time-course experiments using AP20187 to control the activation status of N-ROR1. The Tet-Off doxcycycline-regulated protein expression system enables us to study gene expression alteration under the same cellular background. The overall induction (doxcycycline) and activation (AP20187) experimental schema is illustrated in Figure 3. Samples were taken at four time points (0, 1, 12 and 24 hours after AP20187 treatment) and one control sample in which N-ROR1 expression was suppressed by maintaining the doxycycline treatment. Gene modulation was then evaluated by the HGU133plus2 array from Affymetrix, which includes 54,675 probe sets for 38,500 human genes.

Following the microarray experiments, up-regulated genes with expressions that differed by a factor larger than 1.3-fold were selected and down-regulated genes were chosen with expressions that differed by a factor smaller than 0.7-fold with respect to the control reference. Approximately 2012 individual cDNA elements (4%) exhibited expression increases greater than 1.3-fold in N-ROR1 (c2) cells compared to the control. Approximately 797 individual cDNA elements (1%) exhibited expression decreases smaller than 0.7-fold in N-ROR1 (c2) cells compared to the control. Using the filtered data, we performed a cluster analysis of a microarray time course, illustrating the time for the genes responsive to N-ROR1 activation. The sets of up-regulated genes in activated N-ROR1 (c2) were divided into nine clusters with similar temporal signatures. A total of 89% of gene probes were up-regulated following N-ROR1 activation for 12 hours. Using the MeV EASE analysis tool, we further

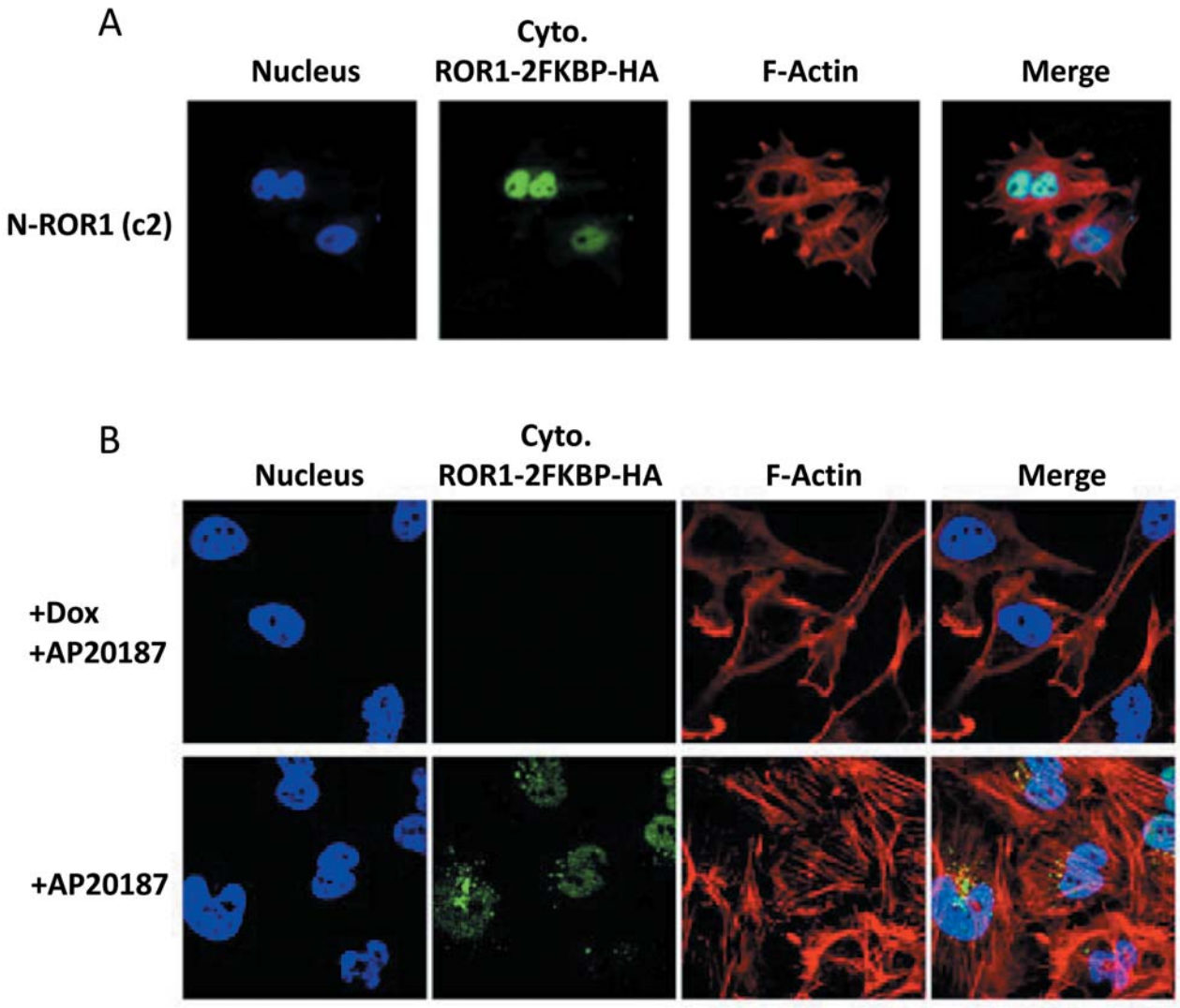

Figure 2. *Expression of N-ROR1 in cells and activation of ROR1 by Ap20187. A: Microscopic analysis of protein localization of ROR1 fusion protein expression in N-ROR1 stable clone (c2). Green pixels correspond to ROR1 staining with anti-HA Ab and anti-mouse IgG-fluorescein isothiocyanate (FITC); blue pixels correspond to DNA labeled with 4',6-diamidino-2-phenylindole (DAPI) and red pixels correspond to F-actin staining. B: Actin organization modulated by ROR1 expression. N-ROR1 (c2) cells were treated with doxycycline to suppress N-ROR1 protein expression and then treated with AP20187 for 3 days (upper panel) or N-ROR1 proteins were activated with AP20187 by removing doxycycline (lower panel). F-Actin cytoskeleton was labeled with rhodamine-phalloidin (red pixels). N-ROR1 expression was labeled with anti-HA ab and anti-mouse IgG-FITC (green pixels). The nucleus was labeled with DAPI (blue pixels).*

annotated the differentially expressed genes in the course of ROR1 expression and activation. Genes involved in cytoskeleton remodeling could found to be up-regulated in this process. To validate this interesting finding, four genes exhibiting up-regulation involved in the regulation of actin cytoskeleton were further analyzed by quantification RT-PCR. Among them, EZR and RDX belong to the ezrin, radixin and moesin (ERM) family of proteins that link the plasma membrane through binding various membrane proteins to the actin cytoskeleton. SOS acts as a guanine nucleotide exchange factor for RAS and RAC, and may target actin filament. CALD1 is a calmodulin and actin-binding protein which stimulates actin binding to tropomyosin and further stabilizes the F-actin skeleton structure. The expression of these genes was clearly modulated by the activation of N-ROR1 (Figure 4).

Nuclear-localized ROR1 influenced cytoskeleton remodeling and motility. Following microarray analyses, activated N-ROR1 up-regulated genes involved in actin cytoskeleton.

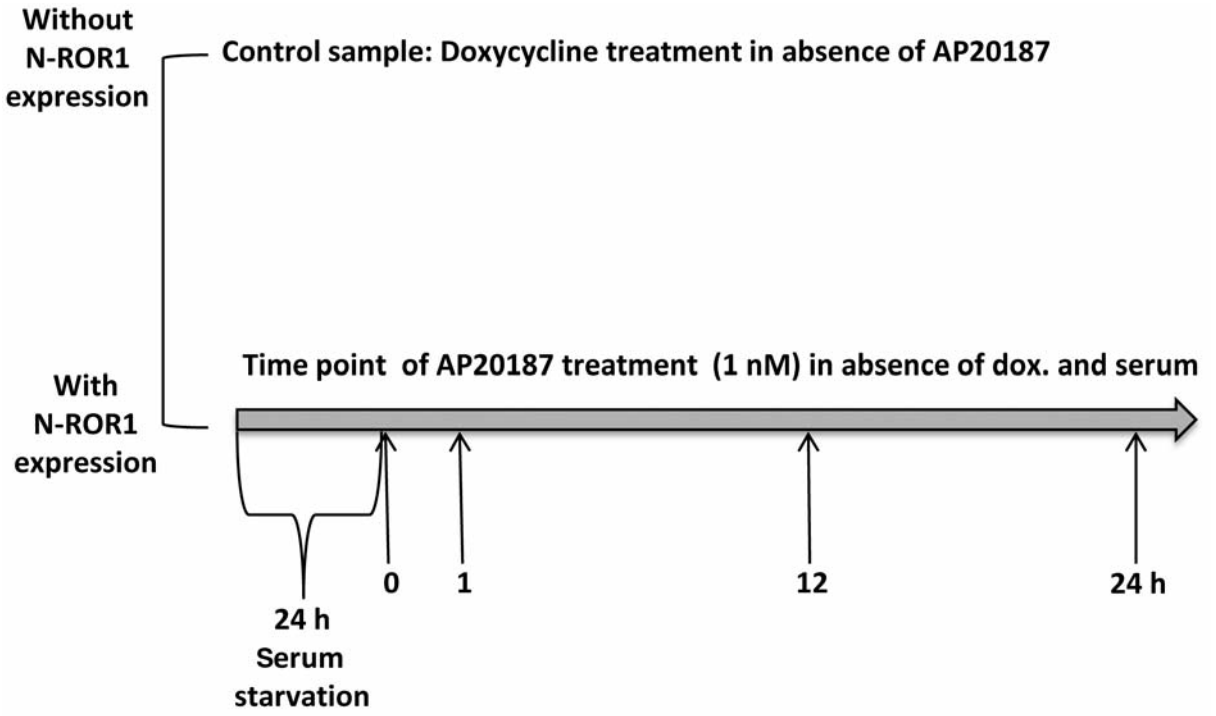

Figure 3. *Experimental design of the time-course analysis of N-ROR1 (c2) cells following AP20187 treatment. Cells were starved of serum for 24 hours before treatment with doxycycline (dox, control) or AP20187. Samples were taken at different time points (0, 1, 12 and 24 hours after AP20187 treatment), and from one control.*

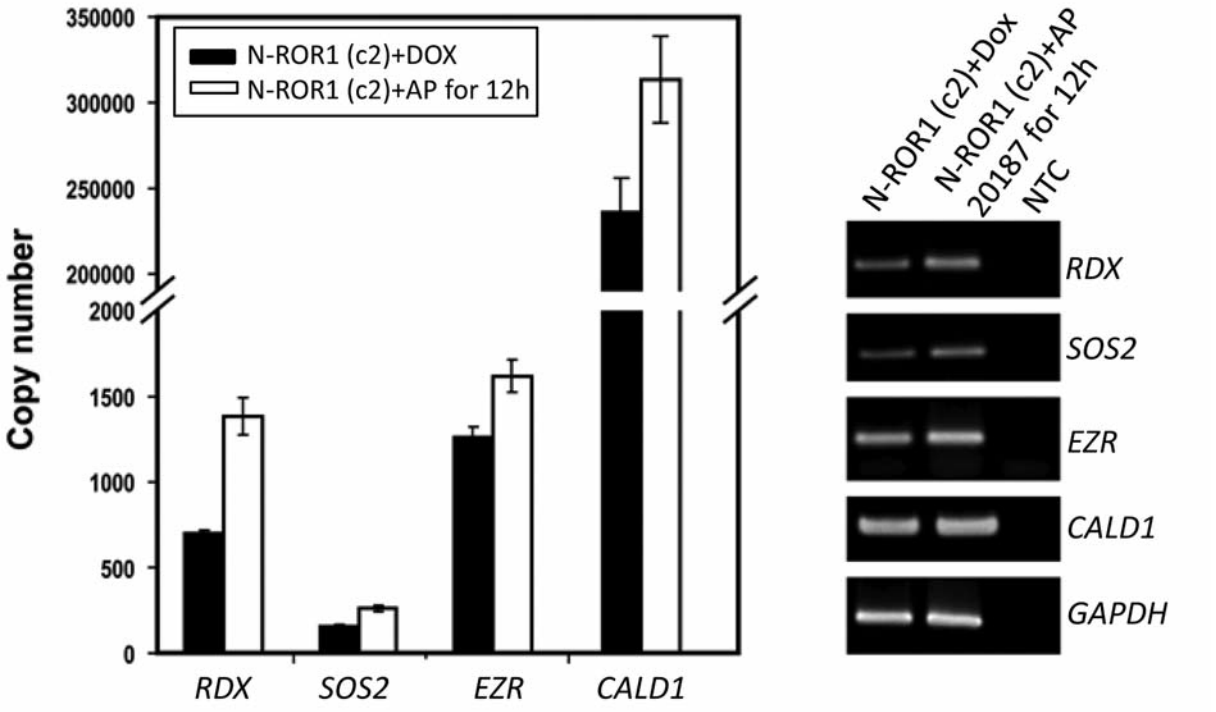

Figure 4. *Expression of radixin (RDX), son of sevenless homolog 2 (SOS2), ezrin (EZR) and caldesmon 1 (CALD1) following N-ROR1 expression. N-ROR1 (c2) cells were treated with doxycycline and AP20187 for 12 hours, respectively, and gene expressions were determined by real-time PCR (left panel) and PCR products separated on agarose gel (right panel). GAPDH was used as control for normalization.*

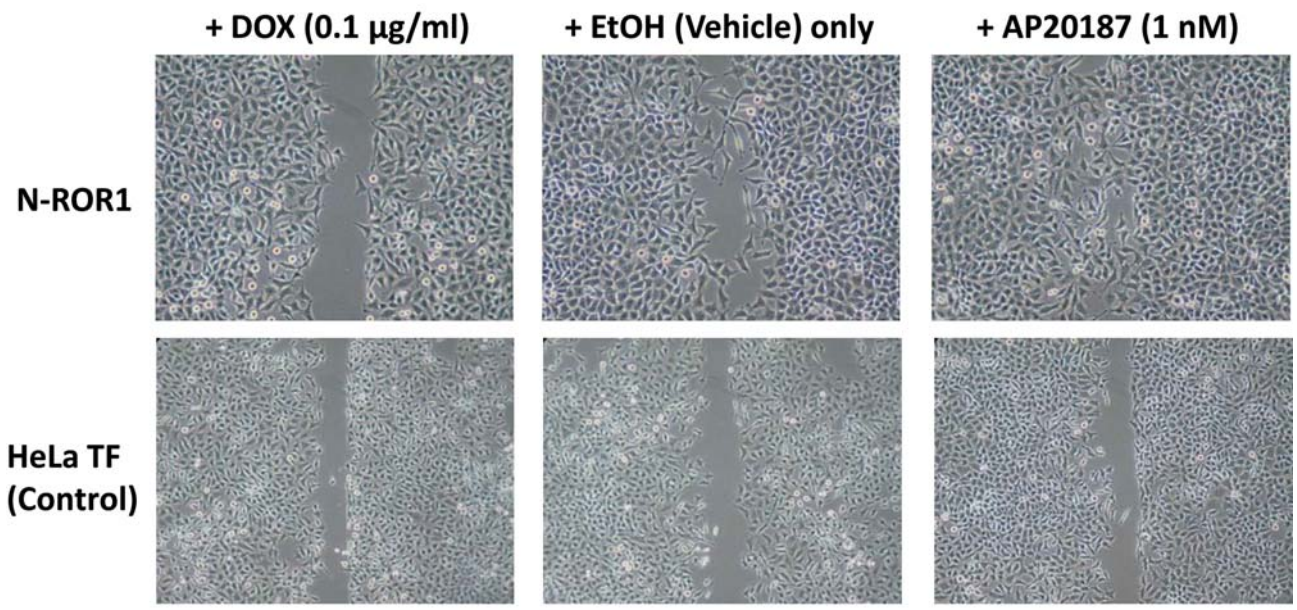

Figure 5. *Cell migration analysis by wound healing assay. N-ROR1 and HeLa TF cells (as control) were grown in monolayers in triplicate in 6-well plates. The cells were treated with doxycycline (DOX), EtOH, and AP20198 separately on day one, and the confluent monolayer was scraped with a sterile tip on day two. The migration into the wounded monolayer was assessed by phase-contrast microscopy 24 h after scraping.*

To investigate the cellular effect of N-ROR1 activation on the actin cytoskeleton, N-ROR1 cells were released from doxycycline to induce the expression of fusion proteins and were subsequently activated with AP20187. Our data showed that release of doxycycline suppression restored full N-ROR1 expression 1.5 days later (data not shown). When N-ROR1 is ectopically expressed in HeLa TF cells, there is a marked difference in actin cytoskeleton architecture. The arrangement of F-actin along the adhesion belt is converted into a radial one by N-ROR1 activation at 1.5 days later. In the presence of N-ROR1, the cells have a large number of actin stress fibers spreading throughout the whole cell that are absent from the control cells. This cell morphological alteration was not a result of the addition of AP20187 itself, as AP20187 alone did not influence the cytoskeleton in the absence of N-ROR1 induction (Figure 2B).

Based on the above results, N-ROR1 is clearly able to mediate actin cytoskeleton remodeling in cells. Since cytoskeleton remodeling can affect the motility and shape of cells, we further investigated the migration patterns of N-ROR1-activated cells. To analyze the effect of migration, control cells and cells with N-ROR1 fusion protein were treated for 24 hours with doxycycline, vehicle control or AP20187. The cells were scraped with a 1-ml tip in the middle of the culture dish and monitored by live cell imaging microscopy. By comparison with the control cells, AP20187-activated N-ROR1 cells exhibited a more advanced migration process. The control parental cells (HeLa TF) did not exhibit a significant change in their cell motility (Figure 5). To further define the cell motility rate following N-ROR1 activation, we measured the displacement rate of N-ROR1 cells using time-lapse videomicroscopy. There were 2,346 displacement measurements in four experimental groups (DOX; DOX+AP20187; EtOH control; AP20187), respectively. We then classified the records into five cell migration levels: (a) 0-0.3 µm/min; (b) 0.3-1 µm/min; (c) 1-2.5 µm/min; (d) 2.5-4 µm/min; and (e) more than 4 µm/min. Based on these five migration levels, we present the percentage bar chart for each of the four groups (shown in Figure 6B). An almost two-fold increase in the average migration rate was observed in activated N-ROR1 cells when compared with non-expressing cells or vehicle-treated cells (1.5 µm/min *vs*. 0.83 µm/min). Finally, we conducted a one-sided Mann-Whitney-Wilcoxon test to determine the significance of N-ROR1 expression on the cellular migration rate. The AP20187 group exhibited significant cellular migration compared with the DOX and DOX+AP20187 groups ($p<0.0001$). This indicates that the cell migration rate was not changed by AP20187 alone in the absence of ROR1 expression (suppressed N-ROR1 expression in doxycycline-treated cells). Interestingly, it was shown that an increased migration rate was also found for the vehicle control (EtOH)-treated cells. It is possible that this could be the result of activation of overexpression of ROR1 tyrosine kinase molecules, which is often observed when protein tyrosine kinase molecules are experimentally expressed. These data

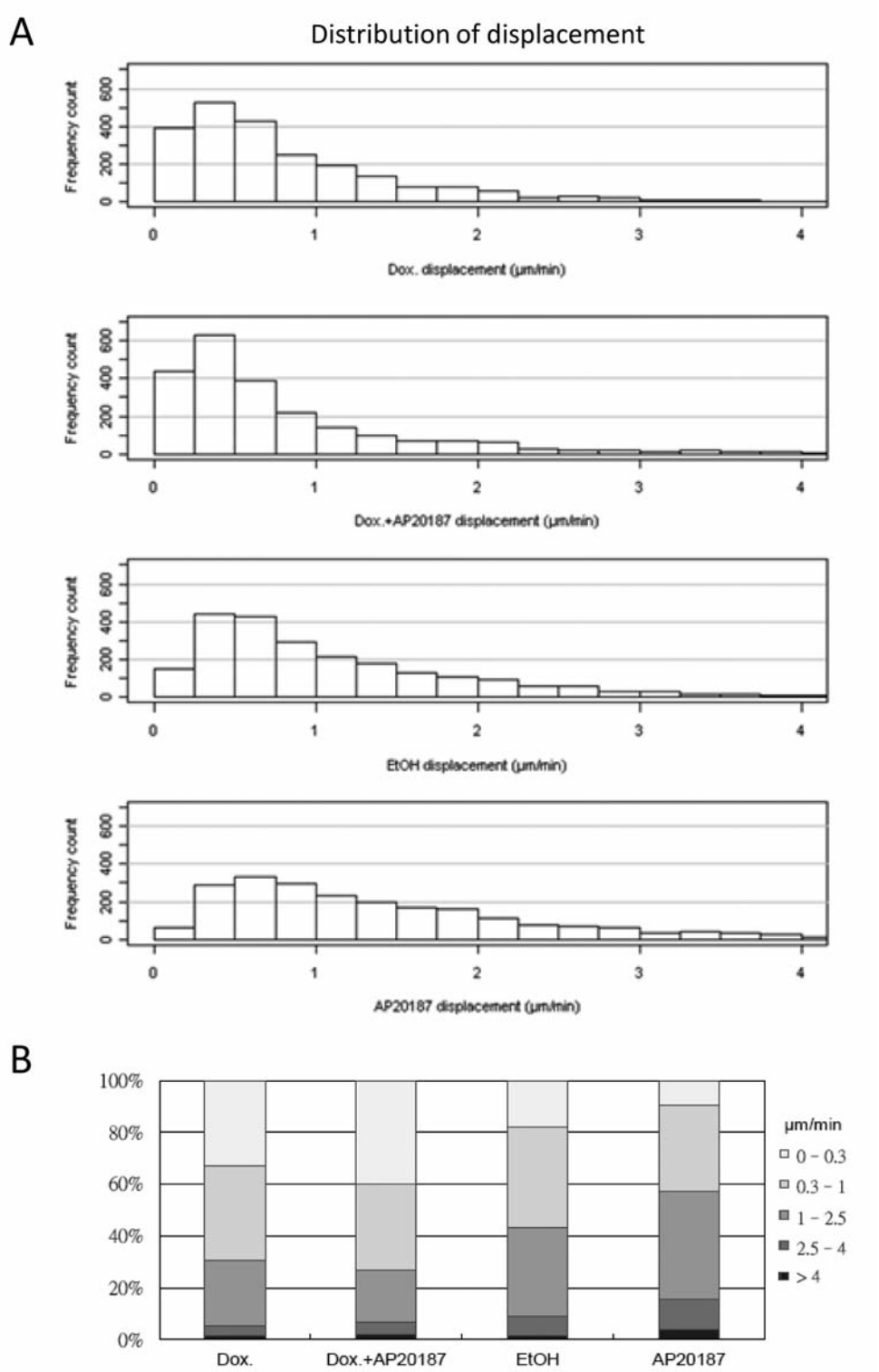

Figure 6. *Increase of cell migration rate following N-ROR1 activation. Cell migration was record using time-lapse video microscopy (Carl Zeiss Axiovert 200M) with cell tracking. Cells were tracked at 15-min intervals for 16 hours and there were 2,346 displacement measures for each experimental group. Velocity is the average speed of the 50 randomly selected cells. A: Distribution of displacements in the four groups. DOX: N-ROR1 cells treated with doxycycline to suppress expression of ROR1. DOX+AP20187: N-ROR1 cells treated with AP20187 activator with the suppression of doxycycline. EtOH: N-ROR1 cells expressing the N-ROR1 protein following the removal of doxycycline and then treatment with ethanol (vehicle control). AP20187: N-ROR1 cells expressing N-ROR1 protein and further activated with AP20187 activator. B: Percentage bar chart. We further classified the displacement records into five cell migration levels for each group: (a) 0-0.3 μm/min; (b) 0.3-1 μm/min; (c) 1-2.5 μm/min; (d) 2.5-4 μm/min; (e) greater than 4 μm/min.*

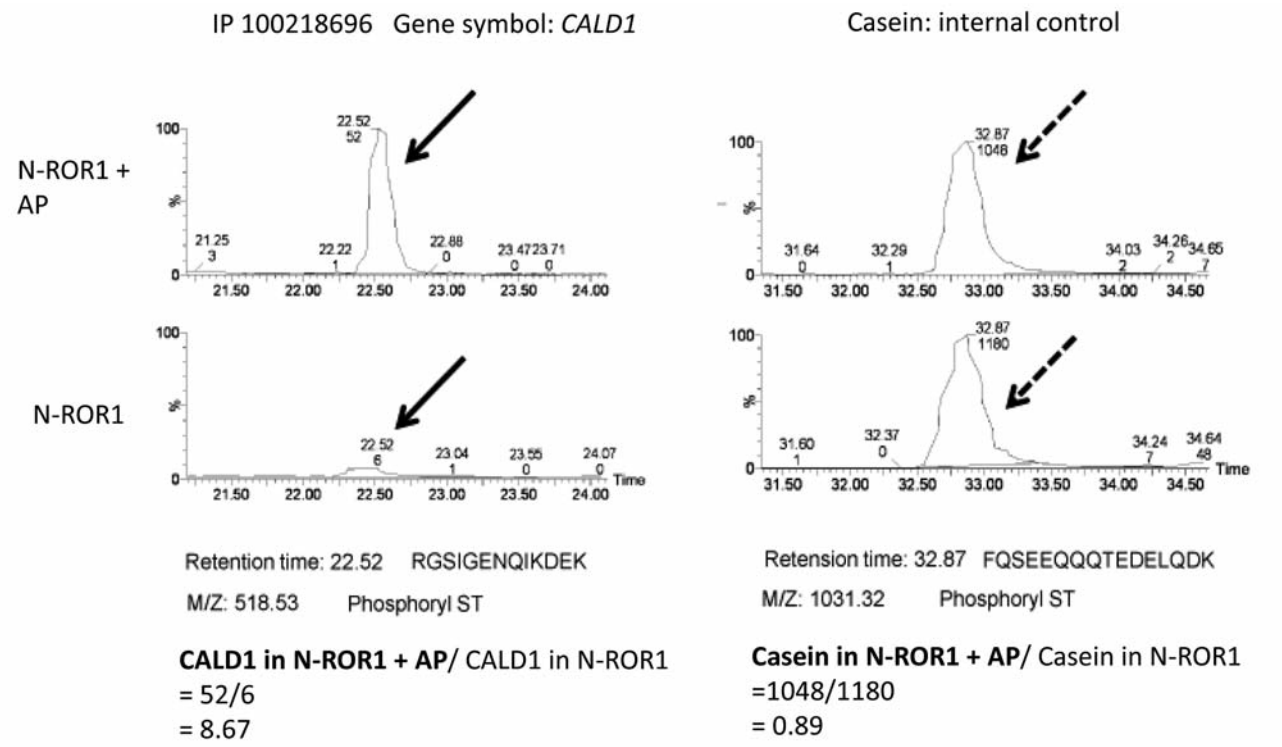

Figure 7. *The phosphopeptides of CALD1 (protein id: IPI00218696) analyzed by LC-MS/MS. The proteins in N-ROR1 (c2) cells treated with AP20187 (1 nM) for 0 and 1 hours were extracted, digested and then the phosphopeptides were enriched using IMAC purification. The upper-left diagram shows the phospho-CALD1 expression in N-ROR1 (c2) cells treated with AP20187 for 1 hour. The peak area is 1667.5 here. The lower-left diagram shows the phospho-CALD1 expression in N-ROR1 (c2) cells without activation. The peak area is 176.4. The arrows indicate the mass chromatographic peak of CALD1 peptide. Bovine beta-casein was added during digestion and its phosphopeptide was used as internal control (right panels). The arrows with dotted line indicate the peak of beta-casein phosphopeptide.*

all suggest N-ROR1 plays an important role in cell migration. In summary, we observed that ectopic expression of N-ROR1 caused dramatic changes in cellular cytoskeleton organization and cellular morphology, as well as cell migration.

Discussion

Accumulated studies reveal that membrane receptor kinases have transactivational function inside the cell nucleus. Nuclear-localized ERBB proteins can function as transcription regulators. Their *C*-terminal regions can execute transactivation activity (10). EGFR protein can target to the A/T-rich sequence (ATRS) in the proximal region of cyclin D1, inducible nitric oxide synthase (iNOS) or aurora-A promoters by interacting with signal transducer and activator of transcription (STATs) (24-26). EGFR protein can also dock with the ataxia telangiectasia and RAD3-related (ATRS) of v-myb myeloblastosis viral oncogene homolog (B-MYB) promoter by associating with E2F transcription factor 1 (E2F1) (27). Therefore, the increased expression of cyclin D1, iNOS, Aurora-A and B-MYB induced by nuclear localized EGFR provides a link between nuclear EGFR and cancer progression.

In our study using a selected N-ROR1 expressing clone, we showed N-ROR1 up-regulates several genes including *EZR, RDX, SOS2* and *CALD1*. Similar findings of this transcriptional modulation were observed using a mixture of N-ROR1-transfected clones (data not shown). This might imply that N-ROR1 affects cytoskeleton remolding and cell migration. CALD1 binds to calmodulin and F-actin, and stabilizes F-actin stress fiber structure (28). Further validation by real-time PCR also confirmed that expression of *RDX, EZR, SOS2* and *CALD1* increased by 2-, 1.3-, 1.7- and 1.3-fold, respectively, following N-ROR1 activation. These molecules act in association with actin filaments in cell membrane and further contribute to cell membrane protrusion (29). Intriguingly, we found that the phosphorylation status of CALD1 was modulated in ROR1-expressing cells by global proteomic analysis (Figure 7). Using LC-MS analysis, we found that expression of Ser202-phosphorylated CALD1 increased by almost 10-fold

following N-ROR1 activation. This increase of phospho-CALD1 was not totally contributed by elevated CALD1 protein expression, which was elevated by 1.2-fold following N-ROR1 activation. It was proposed that CALD1 may be involved in the modulation of cell movement and spreading (30). Therefore, N-ROR1 may regulate expression or activation of genes which function in intermediates of F-actin filament and cell membrane to affect cytoskeleton organization.

Although ROR1 has been implicated in neuron development, its biological role is unknown. In this study, we showed that stable N-ROR1 expression clone exhibited actin stress fiber remodeling and N-ROR1 also affected cell motility. We previously proposed that greater cell migration was driven by cycles of actin reorganization (31). That is, through induction of the pools of genes involved, N-ROR1 is able to regulate cytoskeleton reorganization and to further affect cell motility. This finding is highly related to the known ROR1 function in neurite extension and axonogenesis (13). The physiological significance of ROR1 needs further investigation. This study might be beneficial in future research elucidating the ROR1 biological signaling pathway.

Acknowledgements

This work was supported by research grants from Academia Sinica and National Science Council. The Homodomerization system (pC4-Fv1E vector and AP20187 compound) was kindly supplied by ARIAD Pharmaceuticals Inc.

References

1 Hsu SC and Hung MC: Characterization of a novel tripartite nuclear localization sequence in the EGFR family. J Biol Chem *282*: 10432-10440, 2007.

2 Xie Y and Hung MC: Nuclear localization of p185neu tyrosine kinase and its association with transcriptional transactivation. Biochem Biophys Res Comm *203*: 1589-1598, 1994.

3 Cheng CJ, Ye XC, Vakar-Lopez F, Kim J, Tu SM, Chen DT, Navone NM, Yu-Lee LY, Lin SH and Hu MC: Bone microenvironment and androgen status modulate subcellular localization of ERBB3 in prostate cancer cells. Mol Cancer Res *5*: 675-684, 2007.

4 Feng SM, Muraoka-Cook RS, Hunter D, Sandahl MA, Caskey LS, Miyazawa K, Atfi A, Earp HS and 3rd: The E3 ubiquitin ligase WWP1 selectively targets HER4 and its proteolytically derived signaling isoforms for degradation. Mol Cell Biol *29*: 892-906, 2009.

5 Kilkenny DM and Hill DJ: Perinuclear localization of an intracellular binding protein related to the fibroblast growth factor (FGF) receptor 1 is temporally associated with the nuclear trafficking of FGF-2 in proliferating epiphyseal growth plate chondrocytes. Endocrinology *137*: 5078-5089, 1996.

6 Myers JM, Martins GG, Ostrowski J and Stachowiak MK: Nuclear trafficking of FGFR1: a role for the transmembrane domain. J Cell Biochem *88*: 1273-1291, 2003.

7 Johnston CL, Cox HC, Gomm JJ and Coombes RC: Fibroblast growth factor receptors (FGFRs) localize in different cellular compartments. A splice variant of FGFR-3 localizes to the nucleus. J Biol Chem *270*: 30643-30650, 1995.

8 Bonacchi A, Taddei ML, Petrai I, Efsen E, Defranco R, Nosi D, Torcia M, Rosini P, Formigli L, Rombouts K, Zecchi S, Milani S, Pinzani M, Laffi G and Marra F: Nuclear localization of TRK-A in liver cells. Histol Histopathol *23*: 327-340, 2008.

9 Pillai G, Cook N, Turley H, Leek RD, Blasquez C, Pezzella F, Harris AL and Gatter KC: The expression and cellular localization of phosphorylated VEGFR2 in lymphoma and non-neoplastic lymphadenopathy: an immunohistochemical study. Histopathology *46*: 209-216, 2005.

10 Wang SC and Hung MC: Nuclear translocation of the epidermal growth factor receptor family membrane tyrosine kinase receptors. Clin Cancer Res *15*: 6484-6489, 2009.

11 Tseng HC, Lyu PC and Lin WC: Nuclear localization of orphan receptor protein kinase (Ror1) is mediated through the juxtamembrane domain. BMC Cell Biol *11*: 48, 2010.

12 Masiakowski P and Carroll RD: A novel family of cell surface receptors with tyrosine kinase-like domain. J Biol Chem *267*: 26181-26190, 1992.

13 Paganoni S and Ferreira A: Neurite extension in central neurons: a novel role for the receptor tyrosine kinases Ror1 and Ror2. J Cell Sci *118*: 433-446, 2005.

14 Paganoni S and Ferreira A: Expression and subcellular localization of Ror tyrosine kinase receptors are developmentally regulated in cultured hippocampal neurons. J Neurosci Res *73*: 429-440, 2003.

15 Katoh M: Comparative genomics on ROR1 and ROR2 orthologs. Oncol Rep *14*: 1381-1384, 2005.

16 Yoda A, Oishi I and Minami Y: Expression and function of the Ror-family receptor tyrosine kinases during development: lessons from genetic analyses of nematodes, mice, and humans. J Recept Signal Tr R *23*: 1-15, 2003.

17 Paganoni S, Anderson KL and Ferreira A: Differential subcellular localization of Ror tyrosine kinase receptors in cultured astrocytes. Glia *46*: 456-466, 2004.

18 Rosen MK, Standaert RF, Galat A, Nakatsuka M and Schreiber SL: Inhibition of FKBP rotamase activity by immunosuppressant FK506: twisted amide surrogate. Science *248*: 863-866, 1990.

19 Allocca M, Di Vicino U, Petrillo M, Carlomagno F, Domenici L and Auricchio A: Constitutive and AP20187-induced Ret activation in photoreceptors does not protect from light-induced damage. Invest Ophth Vis Sci *48*: 5199-5206, 2007.

20 Cotugno G, Formisano P, Giacco F, Colella P, Beguinot F and Auricchio A: AP20187-mediated activation of a chimeric insulin receptor results in insulin-like actions in skeletal muscle and liver of diabetic mice. Hum Gene Ther *18*: 106-117, 2007.

21 Kao HW, Chen HC, Wu CW and Lin WC: Tyrosine-kinase expression profiles in human gastric cancer cell lines and their modulations with retinoic acids. Br J Cancer *88*: 1058-1064, 2003.

22 Chen CJ, Tseng MC, Lin HJ, Lin TW and Chen YR: Visual indicator for surfactant abundance in MS-based membrane and general proteomics applications. Anal Chem *82*: 8283-8290, 2010.

23 Wu CW, Li AF, Chi CW, Huang CL, Shen KH, Liu WY and Lin W: Human gastric cancer kinase profile and prognostic significance of MKK4 kinase. Am J Pathol *156*: 2007-2015, 2000.

24 Hung LY, Tseng JT, Lee YC, Xia W, Wang YN, Wu ML, Chuang YH, Lai CH and Chang WC: Nuclear epidermal growth factor receptor (EGFR) interacts with signal transducer and activator of transcription 5 (STAT5) in activating Aurora-A gene expression. Nucleic Acids Res *36*: 4337-4351, 2008.
25 Lo HW, Hsu SC, Ali-Seyed M, Gunduz M, Xia W, Wei Y, Bartholomeusz G, Shih JY and Hung MC: Nuclear interaction of EGFR and STAT3 in the activation of the iNOS/NO pathway. Cancer cell *7*: 575-589, 2005.
26 Lo HW, Xia W, Wei Y, Ali-Seyed M, Huang SF and Hung MC: Novel prognostic value of nuclear epidermal growth factor receptor in breast cancer. Cancer Res *65*: 338-348, 2005.
27 Hanada N, Lo HW, Day CP, Pan Y, Nakajima Y and Hung MC: Co-regulation of B-MYB expression by E2F1 and EGF receptor. Mol Carcinogen *45*: 10-17, 2006.
28 Mayanagi T, Morita T, Hayashi K, Fukumoto K and Sobue K: Glucocorticoid receptor-mediated expression of caldesmon regulates cell migration *via* the reorganization of the actin cytoskeleton. J Biol Chem *283*: 31183-31196, 2008.
29 Bretscher A: Regulation of cortical structure by the ezrin-radixin-moesin protein family. Curr Opin Cell Biol *11*: 109-116, 1999.
30 Lin JJ, Li Y, Eppinga RD, Wang Q and Jin JP: Chapter 1: roles of caldesmon in cell motility and actin cytoskeleton remodeling. Int Rev Cell Mol Biol *274*: 1-68, 2009.
31 Cramer LP, Mitchison TJ and Theriot JA: Actin-dependent motile forces and cell motility. Curr Opin Cell Biol *6*: 82-86, 1994.

Received August 24, 2011
Revised November 7, 2011
Accepted November 8, 2011